



Mini review

3D printing for microsattellites—material requirements and recent developments

Tomasz Blachowicz¹, Kamila Pająk¹, Przemysław Recha² and Andrea Ehrmann^{3,*}

¹ Institute of Physics—Center for Science and Education, Silesian University of Technology, 44-100 Gliwice, Poland

² Faculty of Automatic Control, Electronics and Computer Science, Silesian University of Technology, 44-100 Gliwice, Poland

³ Faculty of Engineering and Mathematics, Bielefeld University of Applied Sciences, 33619 Bielefeld, Germany

* **Correspondence:** Email: andrea.ehrmann@fh-bielefeld.de.

Abstract: Microsatellites for space applications are being intensively investigated in recent years. They can be used for diverse imaging and inspection applications in space, are relatively inexpensive and can be developed fast. Another rapidly emerging class of technologies is 3D printing which can be used to prepare nearly all shapes from diverse polymers, metals and other materials. The intersection between both techniques, however, is still small. Here we give an overview of the first approaches to perform 3D printing for microsattellites and similar space applications, of material requirements for such applications as well as properties of typical 3D printing materials, enabling suggestions for future experiments and pointing out challenges which have to be taken into account.

Keywords: microsattellites; 3D printing, polymer; metal; spacecraft; temperature; irradiation

1. Introduction

Microsatellites have been investigated deeply in experiment and simulation during the last years, especially since they can be built relatively fast and inexpensively [1]. Typical applications of such microsattellites range from earth observation, satellite service and on-orbit inspection to space exploration [2], making sophisticated technology necessary for rendezvous control and navigation [3].

Another challenge of high importance for microsattellites and other spacecraft is related to the

materials which can be used to produce them. On the one hand, heat shields can be used to allow bringing the microsatellite with the included equipment to earth [4]. On the other hand, during their working period, the instruments inside the microsatellite should be kept at standard electronics temperatures around room temperature and for non-operating times in a temperature range of -20 to 50 °C [4], while the outside of the microsatellite may experience much stronger varying temperatures. Besides these durable temperature requirements, depending on the application, solar or cosmic radiation may be of interest.

The second emerging technology taken into account here is 3D printing, also described as rapid prototyping. These wordings mean a broad range of diverse techniques, used for diverse applications [5]. Fused deposition modelling (FDM) is typical for inexpensive desktop printers, allowing printing different polymers which may be filled with other materials [6]. This technique can also be used to prepare composites of 3D printed polymers and textile fabrics, in this way improving the mechanical properties and the production speed, as compared to purely 3D printed objects [7–10]. An older technique is stereolithography (SLA), typically used to prepare polymer or ceramic objects [11] and also capable of being combined with other materials, such as textile fabrics [12]. These and other 3D printing techniques are capable of producing objects of a broad range of polymers, metals, ceramics and composites.

Here, we firstly give an overview of typical recent applications for microsatellites, followed by the corresponding material necessities. Finally, an overview is given of recent studies using 3D printing for different parts of microsatellites.

2. Microsatellite applications

Microsatellites are usually defined by their mass in the range of 10–100 kg, while satellites in the mass range of 1–10 kg are called nanosatellites, and heavier ones in the range of 100–500 kg are named minisatellites [13]. They are launched with a carrier rocket and separated when the intended orbit is reached, often by pyrotechnics, necessitating shock-proof mounting of the equipment in the microsatellite [14].

As mentioned above, microsatellites can be used for a broad range of possible applications, from communication to science, military and/or earth observation [13]. Most recently, Gao et al. used satellite observations for a within-season emergence approach to map crop green-up days by applying data with a high spatial resolution of 10 m and a temporal resolution of 2-day revisits, received from the *Vegetation and Environment monitoring New MicroSatellite* (VEN μ S) for experimental fields in Maryland during the 2019 growth season. Comparing these data with others gained from Operational Sentinel-2 (10 m resolution, 5-day revisit) and routine HLS (30 m resolution, 3–4-day revisit) was used to test the quality of the within-season approach for different temporal and spatial resolutions [15]. Generally, such crop growth stage observations using satellite time series is important, while the use of the pure satellite data is limited. They necessitate diverse image processing steps to deliver sufficient data [16–18] and need to be evaluated at least during one season, normally for longer times to avoid possible misinterpretations of the images [19–21]. Ideally, satellite observations are combined with ground-based evaluations [22–24].

Such optical examinations of the earth can also be used for urban planning, precision agriculture or forestry [25,26], as depicted in Figure 1 [26], as long as undesired temperature variations of the CMOS sensor and similar problems can be avoided [27]. Global navigation satellite system investigations in the radio frequency band can be used to investigate ocean surface wind speed,

surface height, soil moisture, snow depth and other values near the earth surface [28].

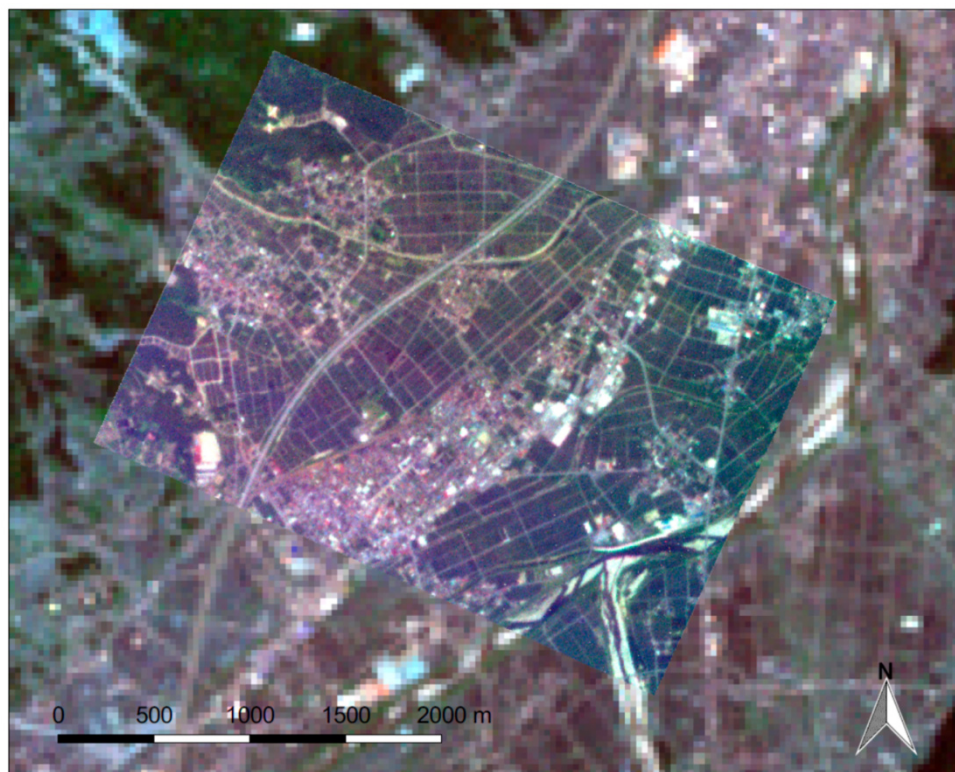


Figure 1. True-color image of the RISING-2 high-precision telescope, overlaying a common composite image of the Landsat 7 Enhanced Thematic Mapper Plus, both taken in 2014 [26].

Another application of microsattellites in low-Earth orbits is the investigation of gravity atmospheric waves, i.e., large-scale air pressure waves between mesosphere and mesopause/thermosphere, e.g., with the “Mesospheric Airglow/Aerosol Tomography Spectroscopy” instrument [29,30]. The Cyclone Global Navigation Satellite System (CYGNSS) mission investigates tropical cyclones in correlation with ocean surface, atmospheric thermodynamics, convective dynamics and radiation [31]. Using an infrared spectrometer, the microsattelite MicroCarb monitors and characterizes CO₂ surface fluxes between carbon sources and sinks [32].

Even lower, in the so-called very-low Earth orbits, i.e. in a height of 250–500 km, microsattellites are launched for communication and Earth observation, in this way enabling size and power consumption of optical and radar instruments, but on the other hand necessitating more power to work against atmospheric drag forces [33].

Diverse scientific experiments, especially in micro-gravity, can be performed using CubeSats, small cubic units which are usually launched on the International Space Station (ISS) or as secondary payloads on launch vehicles [34]. Until 2020, more than 1000 CubeSats were launched into low Earth orbit [35], with several Moon or Mars missions being planned [36]. It should be mentioned that for such interplanetary missions or also de-orbiting missions of space debris, special propulsion technologies are necessary in addition to the material requirements [37]. In 2017, a study categorized CubeSat missions into primary mission objectives such as Earth science, deep space exploration,

heliophysics, astrophysics, spaceborn laboratory, and technology demonstration, indicating that even these specialized microsattellites can be found in nearly all possible applications of small satellites [38].

Magnetospheric studies can be performed, e.g., using one chief microsattellite and several deputy nanosatellites [39,40]. Opposite to Earth observations which are often performed from low-Earth orbits, here highly elliptical orbits are used, causing other necessary properties of the materials used for this purpose.

Clusters of self-organizes connectable microsattellites can go one step further and perform more sophisticated operations, e.g. to hold spacecrafts together, form large array structures such as for a space debris protection net, replace damaged parts temporarily, etc. [41].

As this short overview of recent research shows, diverse applications of microsattellites are possible, necessitating a broad range of material properties which will be evaluated in the next section.

3. Material requirements of microsattellites

In the low Earth orbit (LEO, ~200–700 km), atomic oxygen and ionizing radiation are most problematic, in addition to ultrahigh vacuum, plasma and hypervelocity impacts by micrometeoroids and space debris [42,43]. In very low Earth orbits (VLEO, ~250–500 km), the atomic oxygen fluxes are even higher [33,44]. In a geosynchronous Earth orbit (~36000 km), on the other hand, charged particles and ionizing radiation cause the strongest material degradation [45,46].

For the insulation blanket of the Hubble space telescope, for example, studies found strong degradation of the mechanical strength as well as thickness decrease of fluorinated ethylene propylene films which were attributed to a combination of atomic oxygen, solar flux and thermal cycling [47]. Thermal cycling in LEO usually ranges from approx. –100 to 100 °C [48].

Grossman et al. describe the influence of LEO environment on polymers more in detail. The solar vacuum UV (VUV) irradiation may degrade thermo-optical and mechanical properties of polymers. Ionizing radiation damages electronic components, solar cells and polymers. Vacuum causes outgassing of polymers and thus surface contaminations and reduction of mechanical properties [43]. In their review, they describe the following classes of polymers [43]: Fluoropolymers, such as the aforementioned fluorinated ethylene propylene, are more resistant to atomic oxygen, but more sensitive to UV radiation. Polymers with C–H bonding did not lose mass due to VUV irradiation, while polymers without C–H bonding did. Silicones show much smaller erosion due to atomic oxygen, but tend to outgassing. On the other hand, ionizing radiation or VUV may lead to cross-linking and thus fixate outgassing contaminants. Composites are quite often used, but especially prone to degradation. Grossman et al. mention the possibility to add a silicone-based protective coating as a protection against atomic oxygen.

Metals, on the other hand, are also damaged by atomic oxygen, as well as carbon fibers are [49]. In his review paper, Reddy pointed out that graphite/epoxy composites were eroded by atomic oxygen. Metallized polymer films or organic paints, used for thermal control, are also usually affected by atomic oxygen. Oppositely, metal or metal-oxide coatings can be used for oxygen protection [50].

Additionally, it must be mentioned that not only the material, but also the morphology of 3D printed parts is highly relevant for their mechanical, thermal and other properties. From previous

research of diverse groups it is well-known that FDM printed parts have a relatively low surface roughness, but a high waviness, while parts produced by selective laser melting, selective laser sintering or powder bed fusion show different surface parameters [51–54]. Since all deviations from a perfectly even surface reduce the mechanical properties of an object [55], it may be necessary to reduce the surface roughness and waviness by chemical, thermal or mechanical after-treatments. On the other hand, most 3D printed objects have voids due to their production processes [56–60]. If such voids cannot be completely avoided, they also must be taken into account to evaluate the mechanical and also thermal properties of 3D printed parts for spacecraft.

This brief overview already shows the difficulties which may be expected if 3D printing is used to produce microsatellite parts. Nevertheless, some recent literature reports give first ideas what may be possible when these two emerging technologies are brought together.

4. 3D printing materials usable for microsatellites

Generally, 3D printing for space applications is not unusual since many, if not most objects used in the space industry are custom-made, besides the possibilities to reduce mass and prepare highly complex parts [61]. The special application for parts of microsatellites, however, has not often been reported yet.

Most recently, Li et al. investigated permalloy magnetic shields for fiber optic gyroscopes in spacecraft, produced by selective laser melting (SLM) [62]. SLM belongs to the laser-based 3D printing methods, thus has a high accuracy and can be used to create metal objects. Permalloy, as one of the materials printable by SLM, has a very small coercivity in combination with high permeability, making this material interesting in motors, power transformers and for magnetic shielding. Li et al. produced magnetic shields in a light-weight design by SLM printing and found similar saturation magnetization and coercive fields as gained by conventional processing methods, making this methods promising for magnetic shields in small satellites [62].

An application of 3D printed phase-change materials is described by Zhou et al. [63]. They applied SLM of $\text{AlSi}_{10}\text{Mg}$ to produce a light-weight thermal controller for spacecraft with a mass less than half the one of typical traditional structures.

Ababneh et al. investigated the possibility of 3D printing lightweight heat pipes for the thermal management of solid-state power amplifiers. Such solid-state amplifiers have diverse advantages in comparison to traveling wave tube amplifiers, especially when using GaN as semiconductor, allowing to significantly reduce volume and energy consumption in comparison to traveling wave tube amplifiers. However, the heat flux dissipation of recent thermal management systems is, by approximately two orders of magnitude, too low. In this project, a titanium heat pipe was 3D printed by direct metal laser sintering and could be shown to allow for sufficient heat transport and the possibility to significantly reduce the radiator size and mass [64].

Guo et al. used SLM to manufacture molybdenum and titanium ion optics, i.e. ion engine grids, for electric thrusters in spacecraft. They found that after managing the process of 3D printing molybdenum, the additively manufactured extraction system showed normal functionality in a long-term test and did not show signs of degradations afterwards (Figure 2) [65].

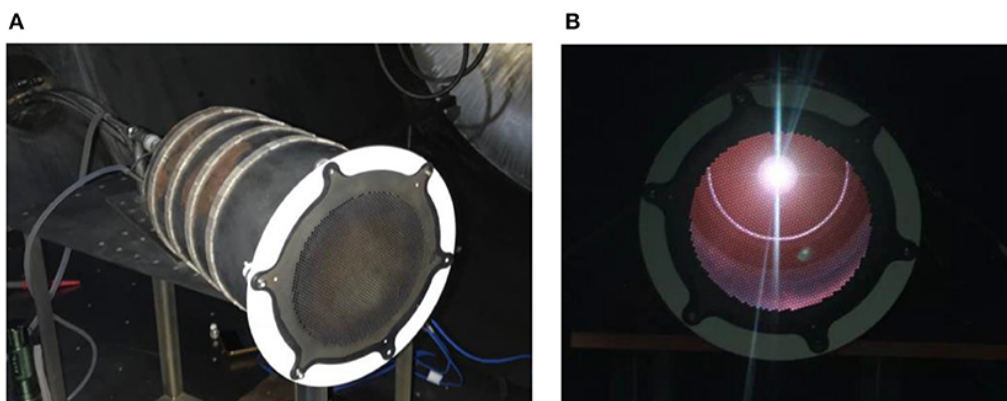


Figure 2. (a) Ion source with screen grid assembly, (b) ion source ignition [65].

A propulsion system based on electrolysis of water was investigated by Harmansa et al. The system consisted of a water container, the electrolysis system with gas storage equipment, and a chemical thruster. In the water storage subsystem, 3D printed propellant management devices were integrated as a proof-of-principle [66].

While the aforementioned applications are planned to be applied inside a satellite or parts of propulsion systems, Abdullah et al. oppositely concentrated on the heat shield and thus one of the parts of a satellite which experience the strongest thermal stress [67]. They 3D printed a composite from carbon fiber and polyether ether ketone (PEEK), a high-temperature printing material. While PEEK can nowadays be printed in special FDM printers, here a laser-based direct energy deposition 3D printer was used, allowing for directly producing a carbon fiber/PEEK composite (Figure 3). These parts were examined in mechanical and arc heating tests in an arc heated wind tunnel, under UV irradiation and by thermal cycles between -70 and 140 °C. Interestingly, this new 3D printed composite material was not significantly influenced by thermal cycles and UV irradiation, showed generally similar properties as conventionally produced carbon fiber/PEEK heat shields, and was thus suggested as a new heat shield material for re-entry flights [67].

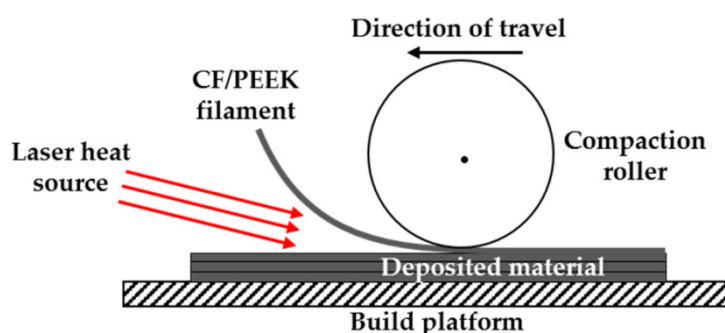


Figure 3. Laser-based direct energy deposition process [67].

Kafi et al. also studied 3D printed heat protection shields [68]. They used different PEEK, polyetherimide (PEI), and poly(ether ketone ketone) (PEKK) filaments for FDM printing, investigated the materials by thermogravimetric analysis and by an oxyacetylene test bed, a method simulating the high heat flux which heat shields have to withstand by putting the samples into an

oxyacetylene flame with a heat flux of 100 W/cm^2 . While all samples experienced a clear mass loss and increased inner temperature during heating for 30 s, only on the outside a char layer was build, while the inner part remained similar to the original state, as visible in Figure 4. The authors found that PEKK had the highest char yield and thus the best ablation performance, while PEI ULTEM 9085 showed the best insulative properties. Generally, all 3D printed samples could withstand the heat flux for 30 s without disintegration, making them promising for future use in heat shields [68].

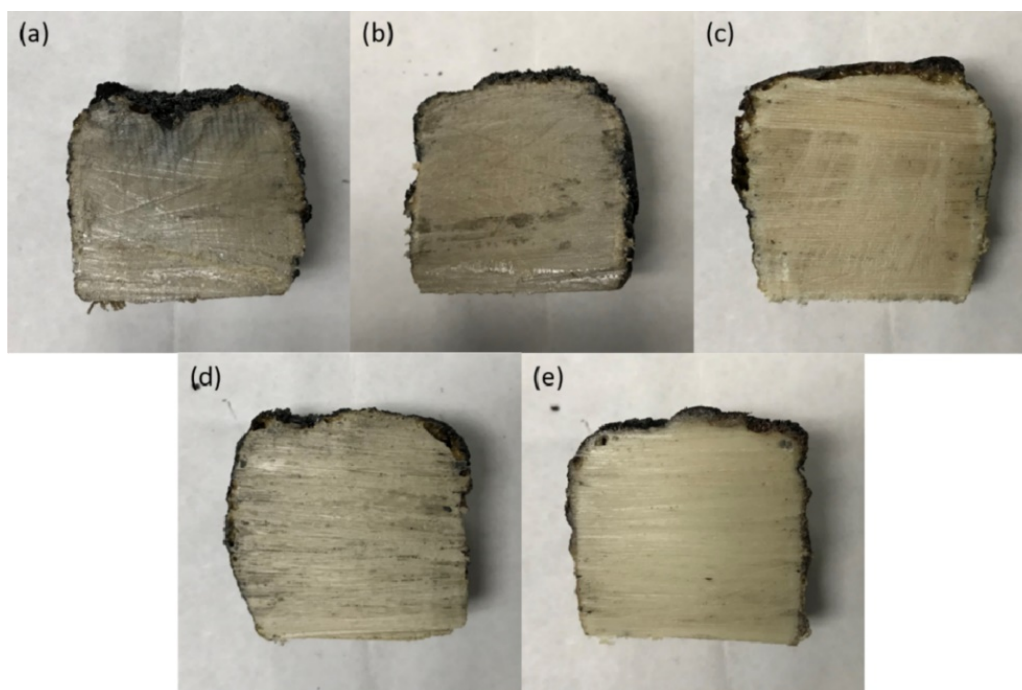


Figure 4. Cross-sections of 3D printed parts after 30 s heat test, as described in the text, from different materials: (a) polyether ether ketone (PEEK) smart materials three-dimensional (3D), (b) PEEK Roboze, (c) polyetherimide (PEI) ULTEM 9085, (d) PEI modified ULTEM 1010, and (e) poly(ether ketone ketone) (PEKK). Reprinted with permission from Ref. [68].

Derusova et al. reported about the first Russian spacecraft containing 3D printed parts, the body of nanosatellite Toms-TPU-120 [69]. They used polyamide 12 (PA 12) for the satellite body, investigated possible defects by laser scanning vibrometry as a nondestructive testing method, and afterwards launched the nanosatellite from the International Space station.

The solar panel of a microsatellite was in the focus of the investigation of Teng et al. Using SLM, they produced a solar panel with a new shape from aluminum alloy (Figure 5) and found increased compression strength, shear strength and reduced weight in comparison with the common honeycomb structure, while at the same time the desired temperature difference necessary for the functionality of the solar panel could be increased [70].

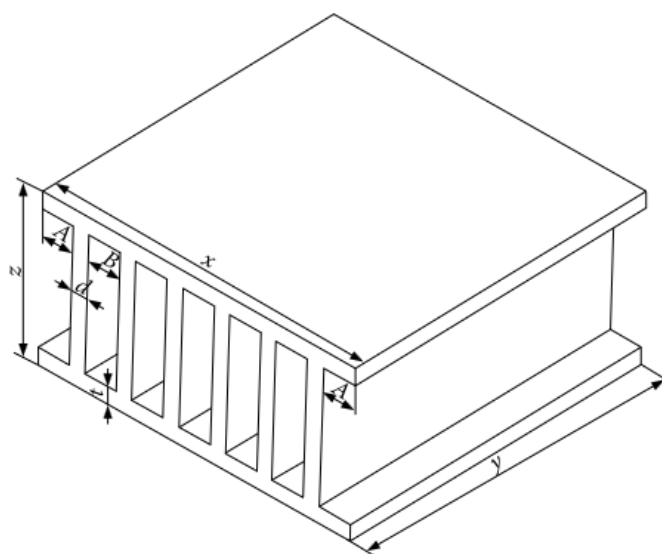


Figure 5. Alternative solar panel structure [70].

Again another aspect was raised by Rossi et al. They combined ideas of passively mitigating the proliferation of space debris with new debris-compliant microsatellite design, enabled by 3D printing. They used an 8U CubeSat as the base configuration and tested 3D printing of the six side panels as well as the shielding by placing the whole nano-satellite in an arc-heated supersonic wind tunnel, resulting in optimization of the debris shields [71].

Absorption of electromagnetic waves in the range of 3.53–24.00 GHz was reached by a 3D printed metamaterial absorber, which at the same time reached larger compressive strength and energy absorption per volume and per mass, as compared to metal lattice cores with identical density [72]. Besides these applications where 3D printing is the core technique, there are many others studies using different 3D printing techniques to produce small parts such as tethers for data transfer or power generation [73], 3D printed waveguide structures [74,75], actuators [76], etc.

5. Conclusion

As this short overview shows, 3D printing has just started to show its possibilities in the broad field of spacecraft and especially microsatellites. While 3D printing nowadays is often recognized as a simple technology, enabling printing gadgets with low-cost FDM printers, the examples here underline that 3D printed objects do not necessarily show reduced material properties, as compared to other production techniques, and on the other hand allow for printing new, sophisticated shapes.

It should be mentioned that while many material-related issues still have to be examined, 3D printing is already starting to find its place in commercial production micro-satellites, rockets and other aerospace objects. The German company EOS GmbH, e.g., offers 3D printing diverse parts of satellites or rockets with various 3D printing techniques [77]. Rocket Lab uses 3D printing to produce rocket engines for the NASA [78]. SpaceX and Blue Origin also use 3D printed parts in valves or engines for spacecraft [79,80]. Even 3D printing of solar panel supports directly in space is planned for the near future [81]. These few examples among many more which made their way from research into commercial application underline the new opportunities offered by 3D printing for

spacecraft, besides the still necessary investigations of new material with enhanced mechanical and thermal properties.

We hope that our mini-review sheds some light on recent challenges and possibilities and stimulates researchers working on microsatellites as well as on diverse 3D printing technologies to join their knowledge, in this way producing next-generation debris-compliant microsatellites.

Acknowledgments

The work was carried out within the Project Based Learning activities by the Silesian Aerospace Technologies Student Chapter funded at Silesian University of Technology through the Research University approach.

Conflict of interests

The authors declare no conflict of interest.

References

1. Chen Y, He Z, Zhou D, et al. (2018) Integrated guidance and control for microsatellite real-time automated proximity operations. *Acta Astronaut* 148: 175–185.
2. Schulte PZ, Spencer DA (2016) Development of an integrated spacecraft guidance, navigation, & control subsystem for automated proximity operations. *Acta Astronaut* 118: 168–186.
3. Delpech M, Berges JC, Djalal, et al. (2012) Preliminary results of the vision based rendezvous and formation flying experiments performed during the prisma extended mission. *Adv Astronaut Sci* 145: 1375–1390.
4. Tuttle S (2014) Thermal design of a recoverable microsatellite. *44th International Conference on Environmental Systems*.
5. Blachowicz T, Ehrmann A (2020) 3D printed MEMS technology—recent developments and applications. *Micromachines* 11: 434.
6. Fafenrot S, Grimmelsmann N, Wortmann M, et al. (2017) Three-dimensional (3D) printing of polymer-metal hybrid materials by fused deposition modeling. *Materials* 10: 1199.
7. Kozior T, Blachowicz T, Ehrmann A (2020) Adhesion of 3D printing on textile fabrics—inspiration from and for other research areas. *J Eng Fiber Fabr* 15: 1–6.
8. Ahrendt D, Karam AR (2020) Development of a computer-aided engineering-supported process for the manufacturing of customized orthopaedic devices by three-dimensional printing onto textile surfaces. *J Eng Fiber Fabr* 15: 1–11.
9. Korger M, Glogowsky A, Sanduloff S, et al. (2020) Testing thermoplastic elastomers selected as flexible three-dimensional printing materials for functional garment and technical textile applications. *J Eng Fiber Fabr* 15: 1–10.
10. Mpofo NS, Mwasiagi JI, Nkiwane LC, et al. (2020) The use of statistical techniques to study the machine parameters affecting the properties of 3D printed cotton/polylactic acid fabrics. *J Eng Fiber Fabr* 15: 1–10.
11. Lu L, Guo P, Pan YY (2017) Magnetic-field-assisted projection stereolithography for three-dimensional printing of smart structures. *J Manuf Sci E-T ASME* 139: 071008.

12. Grothe T, Brockhagen B, Storck JL (2020) Three-dimensional printing resin on different textile substrates using stereolithography: A proof of concept. *J Eng Fiber Fabr* 15: 1–7.
13. Konecny G (2004) Small satellites—a tool for earth observation? *ISPRS Archives XXXV Part B4*: 580–582.
14. Pan XT, Zhang YL, Lu YF, et al. (2020) A reusable SMA actuated non-explosive lock-release mechanism for space application. *Int J Smart Nano Mater* 11: 65–77.
15. Gao F, Anderson M, Daughtry C, et al. (2020) A within-season approach for detecting early growth stages in corn and soybean using high temporal and spatial resolution imagery. *Remote Sens Environ* 242: 111752.
16. Viovy N, Arino O, Belward AS (1992) The Best Index Slope Extraction (BISE): A method for reducing noise in NDVI time-series. *Int J Remote Sens* 13: 1585–1590.
17. Ma M, Veroustraete F (2006) Reconstructing pathfinder AVHRR land NDVI time-series data for the Northwest of China. *Adv Space Res* 37: 835–840.
18. Julita T, Cremonese E, Migliavacca M, et al. (2014) Using digital camera images to analyse snowmelt and phenology of a subalpine grassland. *Agri Forest Meteorol* 198: 116–125.
19. Jönsson P, Eklundh L (2004) TIMESAT—a program for analyzing time-series of satellite sensor data. *Comput Geosci* 30: 833–845.
20. Hermance JF, Jacob RW, Bradley BA, et al. (2007) Extracting phenological signals from multiyear AVHRR NDVI time series: framework for applying high-order annual splines with roughness damping. *IEEE T Geosci Remote* 45: 3264–3276.
21. Zhou J, Jia L, Menenti M (2015) Reconstruction of global MODIS NDVI time series: performance of Harmonic ANalysis of Time Series (HANTS). *Remote Sens Environ* 163: 217–228.
22. Sakamoto T, Wardlow BD, Gitelson AA, et al. (2010) A two-step filtering approach for detecting maize and soybean phenology with time-series MODIS data. *Remote Sens Environ* 114: 2146–2159.
23. Gao F, Anderson MC, Zhang X, et al. (2017) Toward mapping crop progress at field scales through fusion of Landsat and MODIS imagery. *Remote Sens Environ* 188: 9–25.
24. Diao CY (2020) Remote sensing phenological monitoring framework to characterize corn and soybean physiological growing stages. *Remote Sens Environ* 248: 111960.
25. Khorram S, Nelson SAC, Koch FH, et al. (2012) *Remote Sensing*, Berlin: Springer Science & Business Media, 2682–2698.
26. Kurihara J, Takahashi Y, Sakamoto Y, et al. (2018) HPT: A high spatial resolution multispectral sensor for microsatellite remote sensing. *Sensors* 18: 619.
27. Xie XG, Jin G, Xu ML (2019) Thermal design of large-power focal plane components for a microsatellite based on pyrolytic graphite sheet. *Int J Aerospace Eng* 2019: 3683671.
28. Tsai YF, Lin CT, Juang JC (2018) Taiwan's GNSS reflectometry mission—The FORMOSAT-7 reflectometry (FS-7R) mission. *J Aeronaut Astronaut Aviat* 50: 391–403.
29. Larsson N, Lilja R, Gumbel J, et al. (2016) The MATS micro satellite mission—tomographic perspective on the mesosphere, *Proceedings of the 4s Symposium*.
30. Hammar A, Park WJ, Chang SY, et al. (2019) Wide-field off-axis telescope for the Mesospheric Airglow/Aerosol Tomography Spectroscopy satellite. *Appl Optics* 58: 1393–1399.
31. Miller SA, Killough RL, Redfern J, et al. (2018) Delivering hurricane science: data processing review of the CYGNSS mission, *2018 IEEE Aerospace Conference*.

32. Bardoux A, Ledot A, Tauziede L, et al. (2018) Low flux NGP characterisation for microcarb application, *International Conference on Space Optics—ICSO 2018*, International Society for Optics and Photonics, 11180: 111803U.
33. Leomanni M, Garulli A, Giannitrapani A, et al. (2017) Propulsion options for very low Earth orbit microsattellites. *Acta Astronaut* 133: 444–454.
34. CubeSat Database. Available from: <https://sites.google.com/a/slu.edu/swartwout/home/cubesat-database>.
35. Kulu E, Nanosats Database, 2020. Available from: <https://www.nanosats.eu/>.
36. Wall M (2015) Tiny Cubesats set to explore deep space. Available from: <https://www.space.com/29306-cubesats-deep-space-exploration.html>.
37. Leverone F, Cervone A, Gill E (2019) Cost analysis of solar thermal propulsion systems for microsattelite applications. *Acta Astronaut* 155: 90–110.
38. Poghosyan A, Golkar A (2017) CubeSat evolution: Analyzing CubeSat capabilities for conducting science missions. *Prog Aerosp Sci* 88: 59–83.
39. Koptev M, Trofimov S, Shestakov S, et al. (2017) Design and keeping of nanosatellite-based highly elliptical orbit formation. *Adv Astronaut Sci* 161: 1011–1091
40. Koptev MD, Trofimov SP, Ovchinnikov MY (2019) Design and deployment of a tetrahedral formation with passive deputy nanosatellites for magnetospheric studies. *Adv Space Res* 63: 3953–3964.
41. Wang XH, Li S, She YC (2017) Concept design and cluster control of advanced space connectable intelligent microsattelite. *Acta Astronaut* 141: 1–7.
42. Verker R, Bolker A, Carmiel Y, et al. (2020) Ground testing of an on-orbit atomic oxygen flux and ionizing radiation dose sensor based on material degradation by the space environment. *Acta Astronaut* 173: 333–343.
43. Grossmann E, Gouzman I (2003) Space environment effects on polymers in low earth orbit. *Nucl Instrum Meth B* 208: 48–57.
44. Gorreta S, Pons-Nin J, López G, et al. (2016) A CubeSAT payload for in-situ monitoring of pentacene degradation due to atomic oxygen etching in LEO. *Acta Astronaut* 126: 456–462.
45. Anderson J, Smith RE (1994) Natural orbital environment guidelines for use in aerospace vehicle development. *NASA Tech Memo* 4527.
46. Raymond JP, Stassinopoulos EG (1988) Space radiation environment for electronics. *P IEEE* 76: 1423–1442.
47. Jones JS, Sharon JA, Mohammed JS, et al. (2013) Small-scale mechanical characterization of space-exposed fluorinated ethylene propylene recovered from the Hubble Space Telescope. *Polym Test* 32: 602–607.
48. Valer JC, Roberts G, Chambers A, et al. (2013) Development of a reusable atomic oxygen sensor using zinc oxide thick films. *IEEE Sens J* 13: 3046–3052.
49. Li L, Yang JC, Minton TK (2007) Morphological changes at a silver surface resulting from exposure to hyperthermal atomic oxygen. *J Phys Chem C* 111: 6763–6771.
50. Reddy MR (1995) Effect of low earth orbit atomic oxygen on spacecraft materials. *J Mater Sci* 30: 281–307.
51. Kozior T, Mamun A, Trabelsi M, et al. (2020) Quality of the surface texture and mechanical properties of FDM printed samples after thermal and chemical treatment. *Stroj Vestn-J Mech E* 66: 105–113.

52. Zmarzly P, Gogolewski D, Kozior T (2020) Design guidelines for plastic casting using 3D printing. *J Eng Fiber Fabr* 15: 1–10.
53. Kozior T, Bochnia J, Zmarzly P, et al. (2020) Waviness of freeform surface characterizations from austenitic stainless steel (316L) manufactured by 3D printing-selective laser melting (SLM) technology. *Materials* 13: 4372.
54. Kozior T, Bochnia J (2020) The influence of printing orientation on surface texture parameters in powder bed fusion technology with 316L steel. *Micromachines* 11: 639.
55. Suh CH, Jung YC, Kim YS (2010) Effects of thickness and surface roughness on mechanical properties of aluminum sheets. *J Mech Sci Techn* 24: 2091–2098.
56. Wickramasinghe S, Do T, Tran P (2020) FDM-based 3D printing of polymers and associated composite: a review on mechanical properties, defects and treatments. *Polymers* 12: 1529.
57. He QH, Wang HJ, Fu KK, et al. (2020) 3D printed continuous CF/PA6 composites: effect of microscopic voids on mechanical performance. *Compos Sci Technol* 191: 108077.
58. Wang X, Zhao LP, Fuh JYH, et al. (2019) Effect of porosity on mechanical properties of 3D printed polymers: experiments and micromechanical modeling based on X-ray computed tomography analysis. *Polymers* 11: 1154.
59. Block LG, Longana ML, Yu H, et al. (2018) An investigation into 3D printing of fibre reinforced thermoplastic composites. *Addit Manuf* 22: 176–186.
60. Cakar S, Ehrmann A (2021) 3D printing with flexible materials—mechanical properties and material fatigue. *Macromol Symp.* (in press)
61. Sacco E, Moon SK (2019) Additive manufacturing for space: status and promises. *Int J Adv Manuf Tech* 105: 4123–4146.
62. Li B, Zhang L, Fu WQ, et al. (2020) General investigations on manufacturing quality of permalloy via selective laser melting for 3D printing of customized magnetic shields. *JOM* 72: 2834–2844.
63. Zhou H, Zhang XY, Zeng HH, et al. (2019) Lightweight structure of a phase-change thermal controller based on lattice cells manufactured by SLM. *Chinese J Aeronaut* 32: 1727–1732.
64. Ababneh MT, Tarau C, Anderson WG (2019) High temperature lightweight heat pipes for solid-state power amplifier (SSPA) thermal management, *Proceedings of the 2019 Eighteenth IEEE Intersociety Conference on Thermal and Thermomechanical Phenomena in Electronic Systems (ITHERM 2019)*, 656–665.
65. Guo N, Xie K, Sangregorio M, et al. (2019) 3D printing of ion optics for electric propulsion. *Front Phys* 6: 145.
66. Harmansa NE, Herdrich G, Fasoulas S, et al. (2019) Development of a satellite propulsion system based on water electrolysis. *Int J Energ Mater Chem Propul* 18: 185–199.
67. Abdullah F, Okuyaja KI, Morimitsu A, et al. (2020) Effects of thermal cycle and ultraviolet radiation on 3D printed carbon fiber/polyether ether Ketone Ablator. *Aerospace* 7: 95.
68. Kafi A, Wu H, Langston J, et al. (2020) Evaluation of additively manufactured ultraperformance polymers to use as thermal protection systems for spacecraft. *J Appl Polymer Sci* 137: 49117.
69. Derusova DA, Vavilov VP, Druzhinin NV, et al. (2019) Nondestructive testing of CubSat satellite body using laser vibrometry. *Russ J Nondestruct* 55: 418–425.
70. Teng L, Zheng XD, Jin ZH (2019) Performance optimization and verification of a new type of solar panel for microsatellites. *Int J Aerospace Eng* 2019: 2846491.

71. Rossi A, Colombo C, Tsiganis K, et al. (2018) ReDSHIFT: A global approach to space debris mitigation. *Aerospace* 5: 64.
72. Jiang W, Yang LL, Ma H, et al. (2018) Electromagnetic wave absorption and compressive behavior of a three-dimensional metamaterial absorber based on 3D printed honeycomb. *Sci Rep* 8: 4817.
73. Leake S, McGuire T, Parsons M, et al. (2016) Applications of a dynamic tethering system to enable the deep space cam jointed observation bot, *Sensors and Systems for Space Applications IX*, International Society for Optics and Photonic, 9838: 983810.
74. Aguirre F, Schatzel D (2017) High density packaging technologies for RF electronics in small spacecraft. *2017 IEEE Aerospace Conference*.
75. Lucyszyn S, Shang XB, Otter WJ, et al. (2018) Polymer-based 3D printed millimeter-wave components for spacecraft payloads, *2018 IEEE MTT-S International Microwave Workshop Series on Advanced Materials and Processes for RF and THz Applications (IMWS-AMP)*, 1–3.
76. Ellery AA (2017) Space exploration through self-replication technology compensates for discounting in net present value cost-benefit analysis: A business case? *New Space* 5: 141–154.
77. EOS GmbH, Additive manufacturing for aerospace. Available from: <https://www.eos.info/en/3d-printing-examples-applications/aerospace-3d-printing/space-propulsion-satellites>.
78. Winick E (2019) Rocket Lab: The small firm that launched the 3D-printed space revolution. Available from: <https://www.technologyreview.com/2019/06/19/134877/rocket-lab-the-small-firm-that-launched-the-3d-printed-space-revolution/>.
79. Thryft AR (2014) SpaceX reveals 3D-printed rocket engine parts. Available from: <https://www.designnews.com/design-hardware-software/spacex-reveals-3d-printed-rocket-engine-parts>.
80. Sher D (2020) Blue origin 3D printed BE-7 engine confirms capability to land on Moon. Available from: <https://www.3dprintingmedia.network/blue-origin-3d-printed-be-7-engine-testing-confirms-capability-to-land-on-the-moon/>.
81. Walker D (2019) Rocket Lab helping Nasa 3D print spacecraft parts in orbit. Available from: <https://www.nzherald.co.nz/nz/rocket-lab-helping-nasa-3d-print-spacecraft-parts-in-orbit/JA4Q4IZW7IH5GAITZVWYER2JZE/>.



AIMS Press

© 2020 the Author(s), licensee AIMS Press. This is an open access article distributed under the terms of the Creative Commons Attribution License (<http://creativecommons.org/licenses/by/4.0>)